On the development and construction of the Double-Flux Concentrator Trap

THESIS

submitted in partial fulfillment of the
requirements for the degree of

BACHELOR OF SCIENCE
in
PHYSICS

Author :	Thijmen de Jong
Student ID :	s2488477
Supervisor :	Dr. Ir. B.J. Hensen
	M. A. Janse MsC.
2^{nd} corrector :	Prof. Dr. Ir. T.H. Oosterkamp

Leiden, The Netherlands, June 13, 2024

On the development and construction of the Double-Flux Concentrator Trap

Thijmen de Jong

Huygens-Kamerlingh Onnes Laboratory, Leiden University
P.O. Box 9500, 2300 RA Leiden, The Netherlands

June 13, 2024

Abstract

To study gravity on the quantum scale, highly isolated systems are necessary. These systems can be created by levitating small particles. This thesis documents a project in which we attempt to design a magnetic levitation trap using two flux concentrator coils in an anti-Meissner orientation to levitate 50 μm microspheres. A sample holder is designed which ensures the proper alignment of the coils and thermalization of all the superconducting components using a copper base and top plate. We did not manage to successfully levitate the microsphere, because the microsphere itself most likely does not reach the right temperature for it to become superconducting. However, we do succeed at consistently sending high currents (600 mA) into a flow cryostat without breaking the superconducting state of the coils. This proves that the trap has the potential to become successful.

Contents

Chapter 1

Introduction

Gravity is one of the fundamental forces in physics and has therefore been researched extensively. On the quantum scale however, current theories on gravity seem to fall apart. This means we still do not fully understand how microscopic particles behave and interact with each other. Finding answers to the questions on quantum gravity is a hugely exciting subject for the coming decades. Especially as technological advancements steadily move into the quantum realm. Take for example quantum computing or microchips with nm sized components. Gravity on the quantum scale generates minuscule forces and therefore highly isolated systems are needed to be able to detect these forces. To create these systems, microscopic particles can be levitated.

1.1 Motivation

Nowadays there are already several techniques known which are used to levitate particles. These techniques can utilise several different physical forces to trap particles of different sizes and materials. For example acoustic or optical traps can be used. Furthermore electromagnetic forces are also highly suitable for different trap designs to levitate either charged particles using electrical fields or magnetic particles (ferromagnetic or diamagnetic) using magnetic fields.

The acoustic trap is the simplest of all: it utilises two speakers set up in such a way that, when sending the same acoustic signal through both of the speakers, a standing wave in air pressure is created. Styrofoam particles can be trapped between the nodes and anti-nodes [1]. The main

advantage of this setup is that it is easy to achieve and quite cheap. It is, however, not very suitable for accurate measurements. The styrofoam particles suffer from a lot of air resistance and therefore the system is not very isolated. Enacting the experiment in vacuum is, of course, not possible as the acoustic standing wave needs air to form.

A technique which is suitable for accurate measurements are so-called optical tweezers. Since the discovery of the technique by Arthur Ashkin in 1970, several different variations of the tweezers have been developed, but they all use the same principle. Optical tweezers all utilize the radiation pressure of high powered lasers to trap particles with a diameter in the order of 100 nanometer. This method is much more precise than the previously discussed one. The traps are very stiff and such accurate measurements for long amounts of time are possible. The setup, however, is quite complex which of course is a disadvantage[2][3].

Using EM-forces to levitate particles brings a new challenge in the form of Earnshaw's theorem. This theorem states that it is impossible to create a configuration in which point charges exist in a stable configuration solely due to electrostatic interaction with the charges. In other words: you cannot trap electrically charged particles or permanent ferromagnets with a constant field [4]. The solution to this problem is a constantly changing field. Wolfgang Paul was the first to tackle this problem when he developed the quadrupole ion trap, later named after its inventor: the Paul trap. This trap uses four electrically charged poles which are constantly alternating, thus beating Earnshaw's theorem. The resulting alternating electric field creates a restoring force to the middle of the trap for the trapped particles [5]. The advantages of this trap is that it is very versatile in its exact configuration and therefore can be used for multiple purposes.

The same strategy to beat Earnshaw's theorem can be applied to magnetic forces to levitate permanent magnets: alternating the created magnetic field. This can be done on a (relatively) large scale by placing four magnets in such a way that a saddle point in the magnetic field is created. When rotating these magnets, on average, an minimum in the magnetic field is created an such a macroscopic permanent magnet can be trapped: the magnetic Paul trap. This same principle can be done on a much smaller scale with instead of moving permanent magnets, the alternating magnetic field is created by two loops through which an alternating current is sent [6].

These techniques have some disadvantages though. Firstly, you can only trap either electrically charged particles or permanent magnets. This restricts research possibilities. Secondly, due to the need to have alternating fields, especially the magnetic Paul trap can be quite unstable. We will be trying to construct a trap which has the advantages of the acoustic, optical and EM traps, without the described disadvantages. The trap will be relatively simple to build, just like the acoustic trap. The particles trapped are neither electrically charged or permanently magnetized. The disadvantage of the need for alternating field is negated by using constant fields. This is possible after all as Earnshaw's theorem only accounts for ferromagnets, diamagnets (magnets that repel all present magnetic field) can be trapped using constant magnetic fields.

1.2 Goal

We will be using a technique inspired by the one described in [7]. It entails trapping a superconducting microsphere (diameter of 50 μm) at cryogenic temperatures between two coils placed in an anti-Helmholtz configuration. Two identical coils are placed along the same axis with the axis moving through the centre of the coils. A constant opposing current is then sent through the coils. The two resulting opposing magnetic fields will combine into a constant gradient between the two coils. Exactly halfway the two coils the magnitude of the magnetic field is zero. The superconducting microsphere will become a perfect diamagnet because of the Meissner effect and thus will repel the magnetic field created by the coils. The microsphere will then be trapped at the point in space where the magnetic field is zero.

In [7] regular coils are used to create the necessary magnetic fields. In our project, we will use special flux concentrator coils. These coils are designed in such a way that they will create the same magnetic field using a lower current than regular coils. This means we can create a high magnetic gradient while sending low enough currents to be used in a flow cryostat.

1.3 Outline thesis

In this thesis we will discuss the development process of the double-flux concentrator trap. First we will discuss the theoretical background of superconductivity which is the working principle behind the flux concentra-

tor coil and the reason the microsphere will start to levitate. afterwards we will go into detail about the technical challenges of constructing the trap and the measuring techniques used. Lastly the results will be shown. The results of these measurements will be shown and discussed in chapter 4. The thesis will conclude with a discussion of the findings and a conclusion.

Chapter 2

Theory

2.1 Electrical current

Electromagnetic currents can travel through a huge variety of materials. One of the simplest types of conductors are Ohmic conductors. Electromagnetic currents in these conductors are governed by Ohm's law

$$U = IR \tag{2.1}$$

This law shows a linear relationship between the voltage and current for all values. The resistance R is a property of the medium through which the current flows. A simple copper wire is an Ohmic conductor. The resistance of this wire is dependent on its length l, radius r and the resistivity ρ of copper. The resistance can then be calculated using the following formula

$$R = \frac{l\rho}{A} = \frac{l\rho}{\pi r^2} \tag{2.2}$$

The resistivity is a elemental property which is practically constant, though typically decreases for metals when cooling down.

Equation 2.1 does not tell the whole story, as it only holds for constant currents. For oscillating currents, the equation transforms into

$$U = IZ = I(R + iX) \tag{2.3}$$

X is called the reactance and represents the imaginary part of the complex impedance Z. X only acts on complex parts of currents, that is why equation 2.3 reduces to equation 2.1 with a constant current: constant currents have no imaginary part. Only alternating currents have an imaginary part.

As every oscillating system, an alternating current can be described using a complex exponent:

$$V = Ae^{i\omega t+\phi} \tag{2.4}$$

with A the amplitude, ω the angular momentum and ϕ a phase shift. Equation 2.4 gives a real and an imaginary voltage. This will result in a current with a real and imaginary part. The ratio between the imaginary voltage and current is given by the imaginary part of Z. For an ideal coil Z has no real part. It is given by the following formula

$$Z = i\omega L \tag{2.5}$$

L is the inductance of a coil. The theoretical inductance of a coil is given by this equation:

$$L = \frac{\mu_0 N^2 A}{l} = \frac{\mu_0 N^2 \pi r^2}{l} \tag{2.6}$$

Of course, for real coils Z has a real part in the form of the resistance of the wire the coil is wound with [8].

2.2 Superconductivity

Ohm's law as described in equation 2.1 and 2.3 holds for nearly all situations, when considering Ohmic conductors of course. There is, however a group of materials which stop behaving according to Ohm's law. They will instead rapidly lose all of there resistivity when becoming sufficiently cold enough. The temperature at which this happens is called the critical temperature and differs from superconductor to superconductor.

When trying to explain the origin of superconductivity, we need to consider the behaviour of electrons in metals. There are several theories on the behaviour of electrons. In 1957 a conclusive theory on superconductivity was first published. The exact theory and its mathematical proof is quite complicated and beyond the scope of this thesis. We will, however, give a small overview. The superconducting transition happens when electrons form so-called Cooper pairs. These are pairs of electrons with opposing spin and momentum. These pairings are very weak and are easily broken by small thermal vibrations. Electrons have spin $\pm\frac{1}{2}$ and therefore are fermions. Fermions have to adhere to Pauli's exclusion principle: two identical fermions cannot occupy the same quantum state. The Cooper pairs, however, have an integer spin as the two spins of the electrons are added together. This means that these pairs all can occupy the

same ground state.

The Cooper pairs have an energy spectrum: energy states the pairs can occupy as a function of their frequency. In this spectrum there is a gap, a space of energy states the pairs cannot occupy. For the Cooper pairs to be excited from the ground state into a higher energy state, the excitation energy must be sufficiently high to cross the gap. These excitations happen due to interactions with phonons in the crystal structure of the superconductor. If the excitation energy is not high enough due to the thermal energy kT becoming too low, no interactions are possible. This means that the Cooper pairs can flow freely without any energy dissipation and thus without resistance[9][10].

2.2.1 Meissner effect

An important characteristic of superconducting materials is the Meissner effect. The Meissner effect is the total expulsion of all magnetic fields by superconducting materials. This will turn the superconductor essentially in a perfect diamagnet. Superconductors achieve this by generating so-called shielding currents on their surface that exactly counter the external magnetic field. These shielding currents can run indefinitely without losing energy is of course due to the fact that the resistance of the medium is zero. To say that the magnetic field is expulsed entirely from the superconductor is not entirely true. There is a small region along the surface where the magnetic field does penetrate. This is the part of the superconductor in which the surface currents flow. The depth of this region is called the London penetration depth λ_L and is usually in the order of 100 nanometer[11]. In figure 2.1a a schematic overview is shown of the Meissner effect.

When warming the metal up too much, superconductivity will break, simply because the temperature becomes greater than T_c. There is an additional way to break superconductivity. Every superconductor also has a critical magnetic field H_c above which superconductivity will break. How a superconductor reacts to the crossing of the critical field is the basis for a classification of superconductors. There are two types: type-I and type-II superconductors. Type-I superconductors are the most straightforward. When the external magnetic field crosses H_c, all superconductivity is lost and the magnetic field can penetrate the conductor in its entirety. Type-II superconductors behave differently: type-II superconductors have two critical fields. Let's call the two fields H_{c1} and H_{c2} where $H_{c1} < H_{c2}$. When

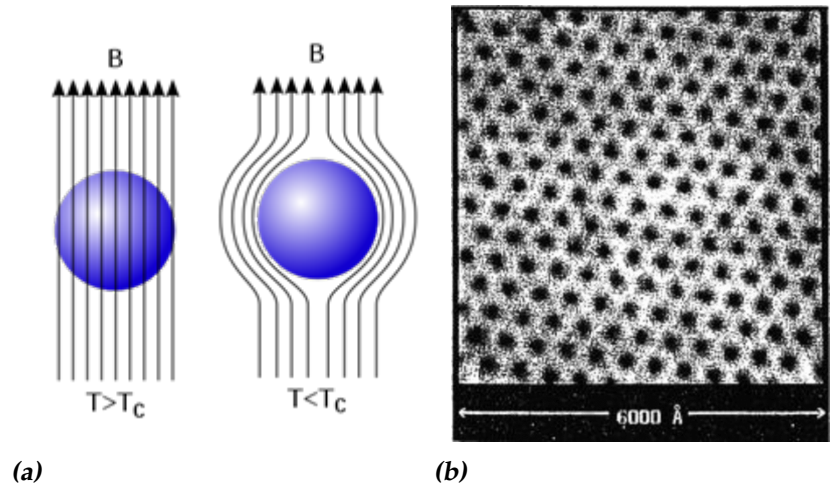

Figure 2.1: *(a): Schematic overview of the Meissner effect. (b): Magnetic vortices in a $NbSe_2$ sample imaged by scanning tunneling microscope. from [12]*

the external field H_0 is greater than H_{c2}, the superconductor loses its superconductivity and will behave normally. However, when $H_{c1}<H_0<H_{c2}$ Singular magnetic flux quanta will start to penetrate the superconductor. These flux quanta will not break superconductivity, but the superconductor is not a perfect diamagnet anymore. A penetrating flux quantum will form a vortex and multiple of these vortices together will form a lattice. In figure 2.1b the vortex lattice in a type-II superconductor can be seen. The critical field is dependent on the temperature of the superconductor:

$$H_c = H_{c0}\left[1 - \left(\frac{T}{T_c}\right)^2\right] \tag{2.7}$$

In this equation H_{c0} is the critical field at 0K [13][12][14].

2.2.2 Superconducting levitation

A setup which strives to stably levitate any particle, needs to create a local minimum in energy potential. Earnshaw's theorem states that this is impossible to do for ferromagnetic particles. However, it does not hold up for diamagnetic particles. This means superconducting materials can be used to make levitating systems only utilizing constant magnetic fields. A simple example can be seen in figure 2.2. In this setup a permanent magnet is placed in a bowl made of superconducting material. The concave shape of the bowl is required to create the potential well in all three dimensions.

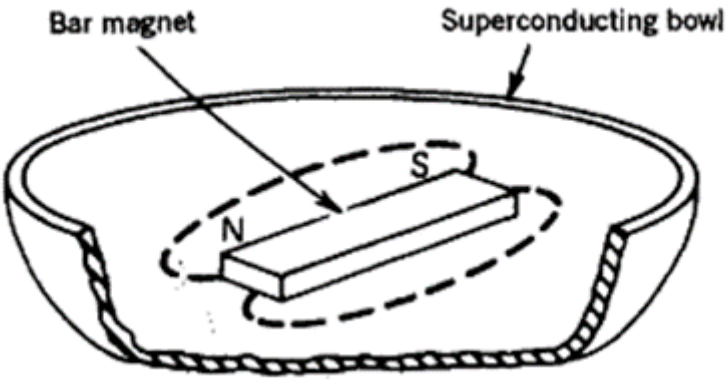

Figure 2.2: *Schematic overview of a simple superconducting levitating system. From [15]*

Due to the Meissner effect, the permanent magnetic field created by the magnet is repelled. This means a force will be applied on the magnet. The same force which is easily felt when trying to push two north poles of two permanent magnets together [15].

This reversed principle will be used in our setup. A minimum in energy potential will be created using two constant magnetic fields. The superconducting diamagnetic microsphere will repel the created magnetic fields and thus experience a force which will push it towards the centre of the trap and confine it in the x,y and z directions.

2.3 Flux concentrator

The aforementioned strong magnetic gradient is generated by the double flux-concentrator. The flux concentrator is a special coil made in such a way that the generated magnetic flux is concentrated through a tiny hole in the center. Because the magnetic flux has to stay constant, the magnetic field through the core of the coils needs to greatly increase:

$$\Phi = \mathbf{B} \cdot \mathbf{S} = BS \tag{2.8}$$

The inner product vanishes because we assume that the magnetic field generated by the coil is perpendicular to the cross section of the coil.

The concentration of the flux is due to the previously explained Meissner

effect. The flux concentrator is made of niobium, a type-II superconductor ($T_c \approx 9K$). The core of the coil is shaped like a funnel and there is a small slit going from the side. This slit is there to force the shielding currents around the core of the coil thus concentrating the field lines through a much smaller area. The funnel shape is there to also concentrate the field lines vertically. A schematic drawing of the flux concentrator can be seen in figure 2.3.

We can calculate the amplified magnetic field generated by the flux concentrator coil. If we assume the length of the coil to be much greater than the radius, the magnetic field generated by a regular coil is given by

$$B = \mu_0 nI = \frac{\mu_0 NI}{L} \tag{2.9}$$

The shielding currents generated have to exactly match the current through the wires of the coil to counter the generated magnetic field. These shielding currents have to flow through the tiny core. This means that when calculating the magnetic field in the core of the flux concentrator, we only have to change L in equation 2.9. Thus the formula for the magnetic field in the core of the flux concentrator coil is as follows

$$B = \frac{\mu_0 NI}{L_2} \tag{2.10}$$

where L_2 is the height of the core as seen in figure 2.3. This means that the amplification due to the design of the flux concentrator is given by the ratio $\frac{L_2}{L_1}$.[16].

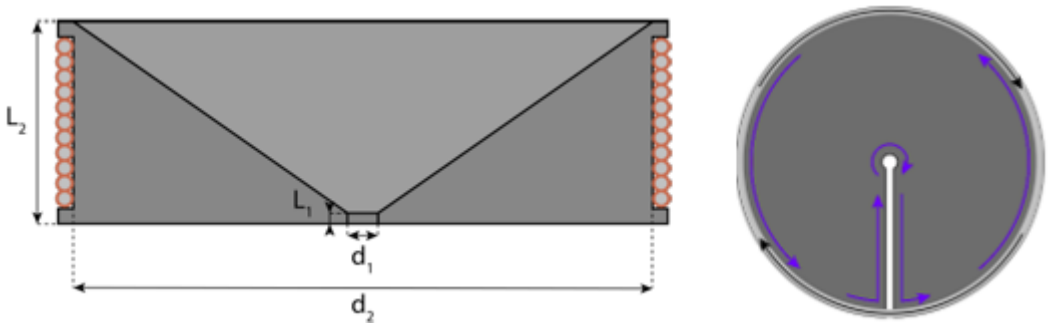

Figure 2.3: *Left: schematic drawing of the cross-section of the flux concentrator. Dimensions are L_1 = 0.474 mm, L_2 = 5.25 mm, d_1 = 0.4 mm, d_2 = 13.15 mm Right: Top down view of the flux concentrator, the blue lines represent the path the shielding currents have to take. Both from [16]*

Chapter 3

Methodology

In this chapter we will go into detail about the technical details of our experimental setup. First we will talk about the design and construction of the sample holder. We will also explain the thermalization of the wire and the trap itself.

3.1 Setup

3.1.1 The sample holder

The sample holder has a few components (visible in figures 3.1, 3.2 and 3.3. These components are: a stand to be placed into the cryostat, two flux concentrators, a circular cover glass, copper foil and an upper plate to tighten the whole stack. A piezoelectric element is glued on top of the top plate. The first flux concentrator is placed on the base such that the 'funnel' is pointing upward. On top of the first concentrator a cover glass is placed. The cover glass is 150 micron thick and has a diameter of 15 mm. On top of the glass, two copper strips with circular ends (100 micron thick, circular end has a diameter of 15 mm) are placed which are screwed on the base. This is for thermalization purposes, which we will go into detail about in the next subsection. A hole (diameter 0.5 mm) is drilled in the center of the circular end in the foils such that they line up exactly with the hole in the flux concentrator. The microsphere (Easyspheres 67/33 SnPb solder spheres, diameter of 50 μm) will be placed inside this hole. In the base and top plate are shallow circular slots present in which the flux concentrators fit exactly. This is done to make sure the holes of the coils are exactly above each other.

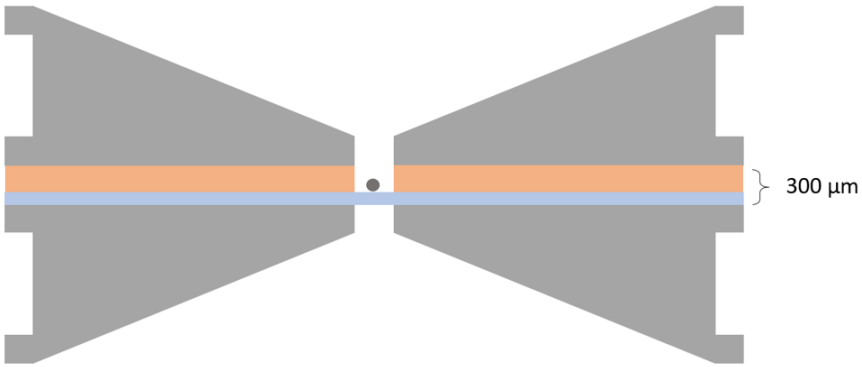

Figure 3.1: *Schematic drawing of the cross section of the experimental setup (not to scale). From top to bottom: the top flux concentrator, two copper thermalization foils, the coverglass on which the microsphere is loaded and finally the bottom flux concentrator.*

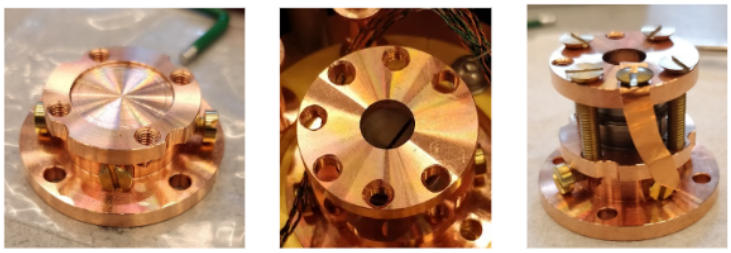

Figure 3.2: *Left: Base of the setup. Middle: Top plate of the setup (without the piezo). Right: The entire set up assembled including thermalization foil for the top plate*

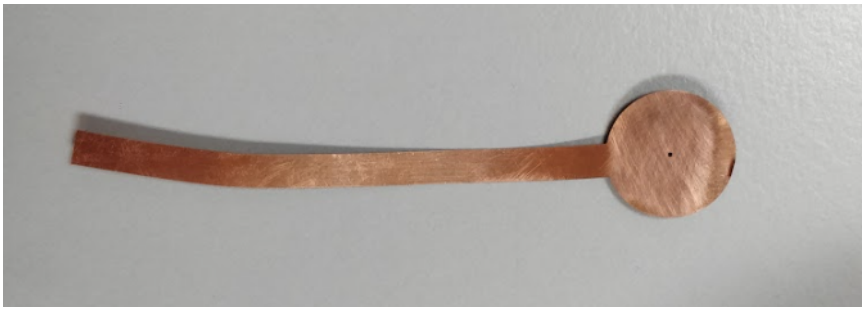

Figure 3.3: *Thermalization foil for the microsphere*

The coils of the flux concentrators are wound with NbTi/CuNi wire with a formvar coating. We tried two different wires with different thickness. Our first attempt was to use the thinnest wire possible to have as many windings as possible. This wire had a thickness of 69 μm. The resulting coils had 700 windings. To prevent electrical shorts, we first wound a piece of teflon tape around the coils. This tape is an electrical insulator, so even if some of the formvar coating would be chipped away, no short would occur. The coils had a total resistance of 6 kΩ. The high resistance is caused by the tiny radius of the wire and the high total length of the wire which made up the coil (30 meter, equation 2.2). This resistance proved to be too high as these coils had a residual resistance when in superconducting state of 20 Ω. This meant that we could only send 6 mA before the superconducting state would be broken due to Joule heating.

Our second attempt was to use thicker wires, namely NbTi/CuNi wire with a diameter of 100 μm This had the following advantages compared to the thin wire: Firstly, the coil had a lot less resistance, caused by a higher radius and a smaller total length of the wire making up the coil. Secondly, the thicker wire is sturdier. We suspected that the thin wire could get pinched or damaged in the winding process. This would create impurities which would result in the high residual resistance. With the thicker wire these impurities occur less. The resulting coils wound with the thicker wire have 180 windings, a resistance of 28 Ω and an inductance of around 360 μH

3.2 Flow cryostat

To reach the temperatures needed for the necessary components to reach superconductivity, the experimental setup will be placed inside a flow cryostat. The flow cryostat used is the ST-500 by Lake Shore Cryotronics. This cryostat uses liquid helium to reach a temperature of 4.5K. The liquid helium is pumped through a capillary running through a gold plated copper mounting block before exiting the cryostat. This way, the flowing liquid helium cools the copper mount and any other samples securely mounted to it. The interior of the cryostat has to be a vacuum before cooling down ($P \approx 1 \cdot 10^{-4}$ mbar). It takes around 10 to 15 minutes to cool down to its minimal temperature of 4.5K. The technical details and exact user manual are given in [17].

3.2.1 Thermalization

When the wires enter the cryostat, they are still room temperature and still have some resistance. This will cause the wires to generate heat when sending current through them. This is called Joule heating:

$$P = VI = I^2R \tag{3.1}$$

Because the inside of the cryostat is a vacuum, everything inside the cryostat we would want to cool down has to be in proper thermal contact with the copper base. One way to make sure everything is properly thermalized, is to use a heatsink. In our setup a copper bobbin is used (figure 3.4. It is in thermal contact with the cryostat and around it the feeding wires are tightly wound. The wires can then dump their heat via the bobbin to prevent them from warming up the sample. To keep the wires in place, the wound bobbins are covered in stycast. The bobbin is screwed onto the bottom of the cryostat. There are two of these heatsinks present for both feeding wires of the flux concentrators. This feeding wire is thicker than the wire which is used to wind the flux concentrator coils. This is done to minimize the resistance of the 'normal' conducting part of the wire and thus minimize joule heating. We chose NbTi/CuNi wire with a diameter of 360 μm. We chose for a CuNi coating over a Cu coating, because it would cause less thermal load provided the wire was quite long. The feeding wire we use is 1.2 m long and wound up to make it fit inside the cryostat.

To thermalize the coils themselves copper is also used. The bottom one is in tight contact with the stand. This stand is made out of solid copper thus the heat of the bottom flux concentrator can escape relatively easily. The top coil is not in direct contact with the bottom one, so to thermalize it an additional copper plate is used. Strips of copper foil are then screwed onto both the top plate and the stand. Through these strips the heat can flow away. Additionally, brass screws are used instead of steel ones as brass is a better heat conductor than steel.

Lastly the superconductor microsphere has to be thermalized too, this is what the strip of copper foil between the coverglasses is for. While cooling the setup down, the microsphere will be in contact with the foil due to Van der Waals forces and as such will be thermalized.

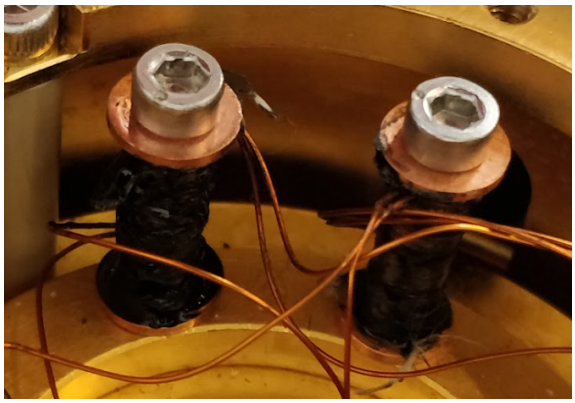

Figure 3.4: *Thermalization bobbins installed in the flow cryostat*

3.3 Superconducting measurements

Before we could do our levitation tests, we had to confirm all the components of the setup would become superconducting. The flow cryostat has an integrated thermometer with which we measured the temperature inside the cryostat. However, even if the temperature would be lower than T_c of the different components, this is no guarantee that the wire and coils are sufficiently thermalized to reach superconducting temperatures. To get clear proof of superconductivity we measured the properties which would change when the components would become superconducting.

3.3.1 Lock-in amplifier

The first way to test whether the wires and coils reached a temperature below T_c was to use a lock-in amplifier (Stanford Research Systems SRS380) to indirectly measure the resistance of the wires and the inductance of the coils. A lock in amplifier is essentially a very precise function generator combined with a voltage meter which can measure the real and imaginary part of the voltage separately. To be able to measure the imaginary part of the voltage is crucial because the inductance only affects the imaginary part of an alternating current. When wire becomes superconducting, it loses its resistance. Thus a simple resistance measurement is sufficient to prove whether the wire becomes superconducting or not. To prove the superconducting transition of the coils, we use the fact that the radius of the coils essentially shrink when becoming superconducting due to the Meiss-

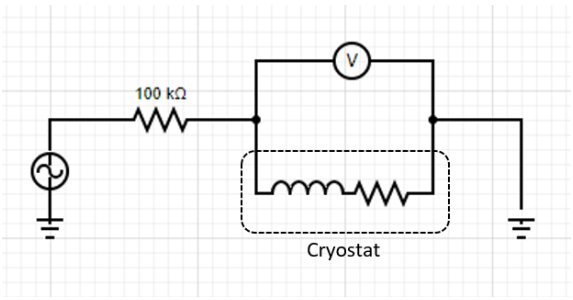

Figure 3.5: *Schematic overview of the electrical circuit used with the lock-in measurements*

ner effect. This shrinking of the radius causes the inductance of the coil to drop (equation 2.6).

A schematic overview of the circuit used to measure is shown in figure 3.5. It is quite a simple circuit: we use the lock-in amplifier to send a alternating signal (amplitude: 1 V, frequency: 1 kHz) through the flux concentrator coil in the cryostat. An additional resistance of 100 kΩ is placed in series. This is done to minimize the increase of current resulting from the resistance of the coil disappearing due to the superconducting transition as well as ensuring the cutoff frequency $\omega_c = \frac{R}{L}$ is much higher than the measuring frequency. This means that any change in measured real and imaginary voltage only results from the superconducting transition of the wire and core respectively. This voltage is measured by the same lock-in amplifier.

3.3.2 Hall Sensor

We used a second method to measure the superconducting transition in which a Hall effect sensor is used to measure the change in magnetic field due to the concentration of the magnetic field.

The Hall effect is the phenomenon where flowing electrons are deflected due to a present magnetic field and therefore create a charge difference in the material through which the current flows. This charge difference in turn creates a voltage which is measured by the Hall effect sensor. The higher the magnetic field in which the sensor is placed, the higher the measured voltage. The output voltage as function of the magnetic field is essentially linear

We mounted the Hall effect sensor on top of the bottom coil in such a way that the magnetic centre was exactly above the hole of the flux concentrator. The coils was placed inside the flow cryostat. We used the Advanced Sensor Technologies HE144. First we measured the output voltage at room temperature at different currents to see the behaviour of the sensor in normal conditions. Afterwards we cooled down to superconducting temperatures did a sweep over the same currents to compare the results to the room temperature findings. As the output voltage as function of the magnetic field is essentially linear, we could compare the measured voltages without calculating the actual magnetic field. Important to note, however, is that we do not know whether the calibration at room temperature is still valid at 4.5 K.

3.4 Levitation tests

With the superconducting tests being completed, we could continue with actually attempting to levitate the microsphere. Before we could do this, we had to load a microsphere in place. To do this, we used a needle on a stage with which we could very accurately move the needle. Due to the small weight of the microsphere the Van der Waals forces between the needle and the microsphere are strong enough that the microsphere can be picked up with the needle. We placed the microsphere either on the bottom cover glass or stuck it to the side of the hole on the copper thermalization foil.

To levitate the microsphere, we cooled down the entire setup. When the desired temperature was reached, we sent currents through the flux concentrator coils using to Tenma current generators. To ensure an anti-Helmholtz configuration was achieved, the correct direction of the current was determined using a Gauss-meter. We sent as much current possible before heating up too much and breaking the superconductivity of the wires. To knock loose the microsphere from either the foil or the glass we used the piezo-element glued to the top of the sample holder. To power the piezo-element we used a wave generator and amplifier to send a sinusoidal wave with with an amplitude of 15 V. We swept the frequency from 100 kHz to 800 kHz. The microsphere was imaged using a microscope with a camera mounted on top (figure 3.6a. We used an objective with an optical magnification of 10. The images in figure 3.7 are made using this optical setup.

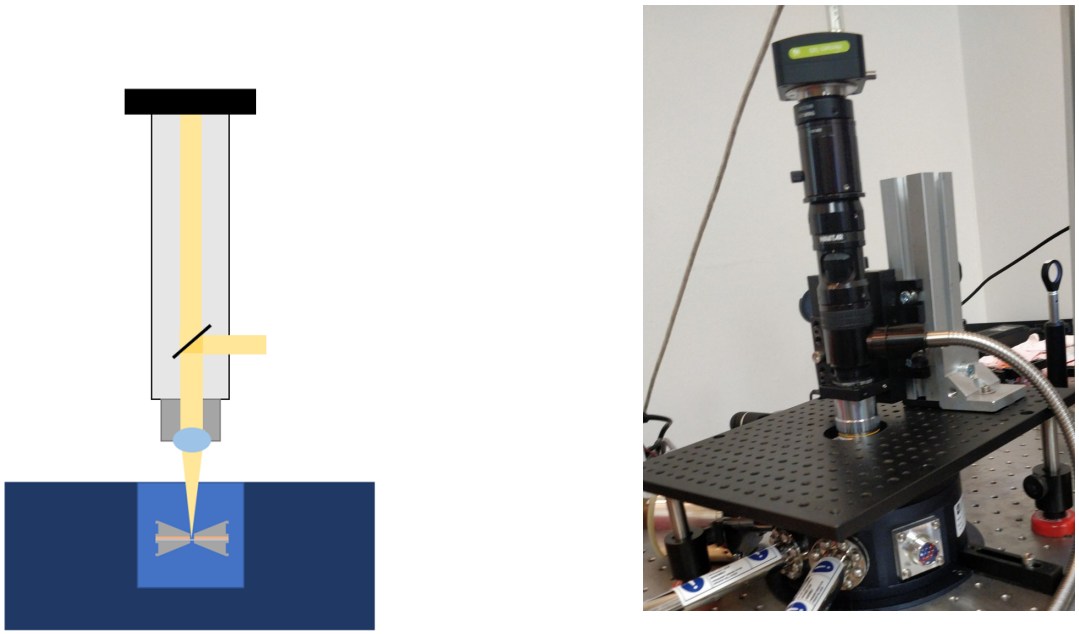

(a) ***(b)***

Figure 3.6: *(a):Schematic overview of the optical setup. Light is brought in with an optical fiber. It is redirected downward through the objective into the flow cryostat (the light blue part) with a beam splitter. At the top of the column a camera is mounted to be able to record the imaged microsphere. (b): picture of the optical setup mounted over the flow cryostat.*

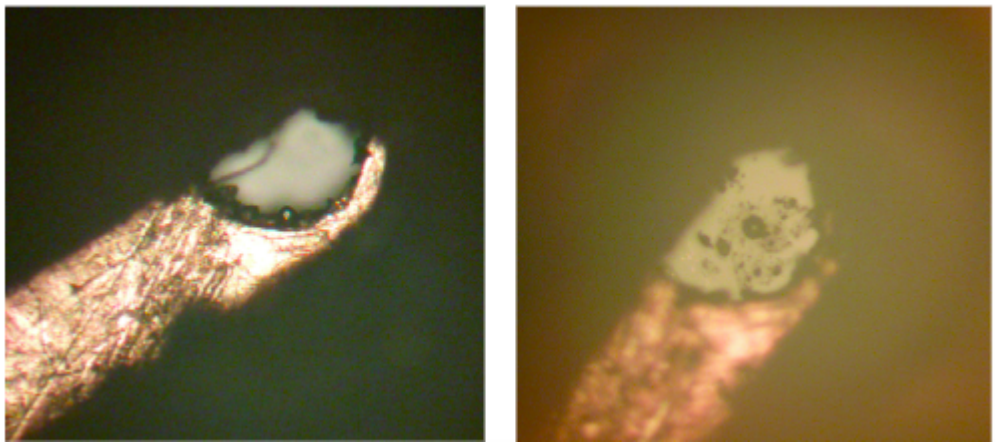

Figure 3.7: *Left: microsphere loaded to the side of the copper foil. Right: microsphere loaded on the cover class*

Chapter 4

Results

In this chapter we show the results of the measurements described in chapter 3. We will first look at the results of the lock-in and Hall-sensor measurements, after which we will describe the results of the actual levitation attempts.

4.1 Lock-in measurements

As stated before in chapter 3, we used two variants of the flux concentrator coil, one with thin wire and one with (relatively) thick wire. The ones with thin wires were proven to be unusable because the critical current was too low. This is visible in figure 4.1. It is clear that when sending

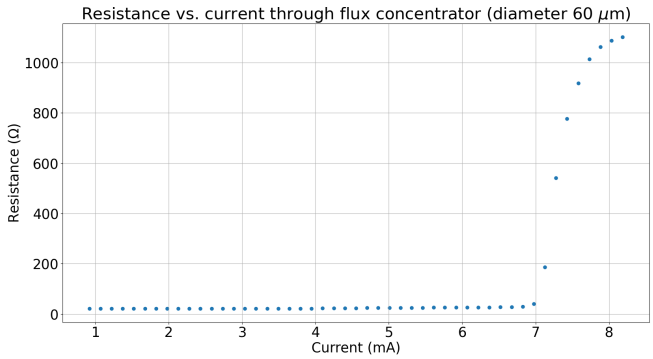

Figure 4.1: *Data obtained by slowly ramping the current through the flux concentrator coil until the wire was no longer superconducting.*

more than 7 mA, the superconducting state is broken and the resistance

of the coil increases to 1000 Ω. The same measurement done with the coils with thicker wire gave a significantly higher I_c as visible in figure 4.2. This figure shows that when sending a very large current of 1 A the resistance of the coil is still only 1.47 Ω. There is an abrupt jump in resistance visible, which most likely means a local loss in superconductivity. This small increase in resistance, however, does not result in a total loss of superconductivity. This means the wire is thermalized well enough to make sure the generated heat due to the additional resistance is conducted away properly. We found that when actually using the coils for longer amounts of time during the levitation tests, we could send up to 600 mA without warming up enough to break superconductivity. Due to the large difference in I_c, we chose to use the coils with thicker wire for the rest of the measurements.

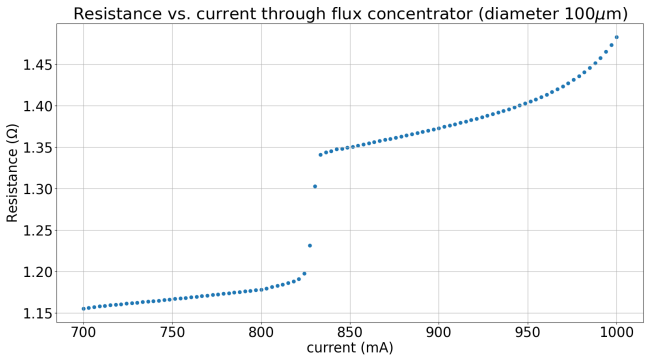

Figure 4.2: *Data obtained by sweeping the current through the flux concentrator coil from 700 mA to 1000 mA. Note that the y-axis only spans from 1.15 Ω to 1.5 Ω as opposed to the kΩ range presented in figure 4.1. There is a small jump in resistance visible but only of 0.15 Ω. This hints at a local break in superconductance but the wire as a whole stays in superconducting state.*

We measured the real and imaginary voltage over the flux concentrator coils every time we cooled down. The measured voltages are shown in figures 4.3 and 4.4. Both the real voltage and the imaginary voltage behave as expected during the cooldown. The measured behaviour of the real voltage during the cooldown first shows a gradual decrease in resistance. This is typical for most metals when cooling down. When the temperature is low enough and $T < T_c$, the voltage and therefore the resistance drops abruptly. This abrupt drop shows the superconducting transition of the wire. Similarly, the abrupt drop of the imaginary voltage shows a drop in inductance of the coil. This might be proof of a superconducting transition of the niobium coil.

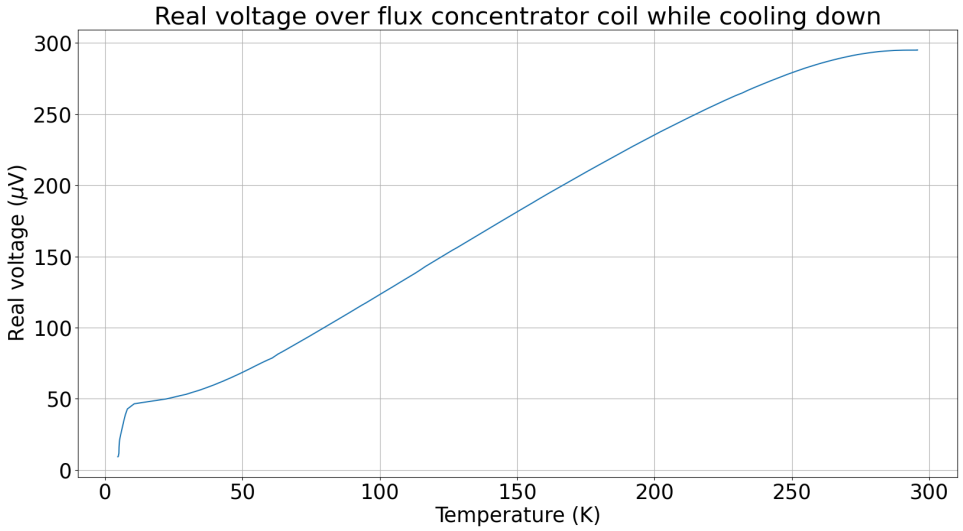

Figure 4.3: *The superconducting transition of the NbTi wire as shown by the sudden drop of real voltage over the coil.*

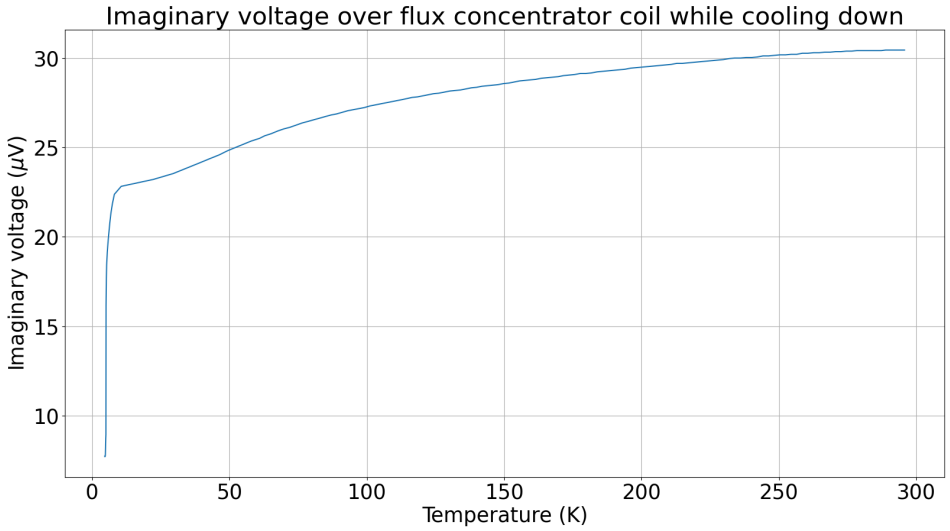

Figure 4.4: *The superconducting transition of the Nb flux concentrator coil as shown by the drop of imaginary voltage over the coil*

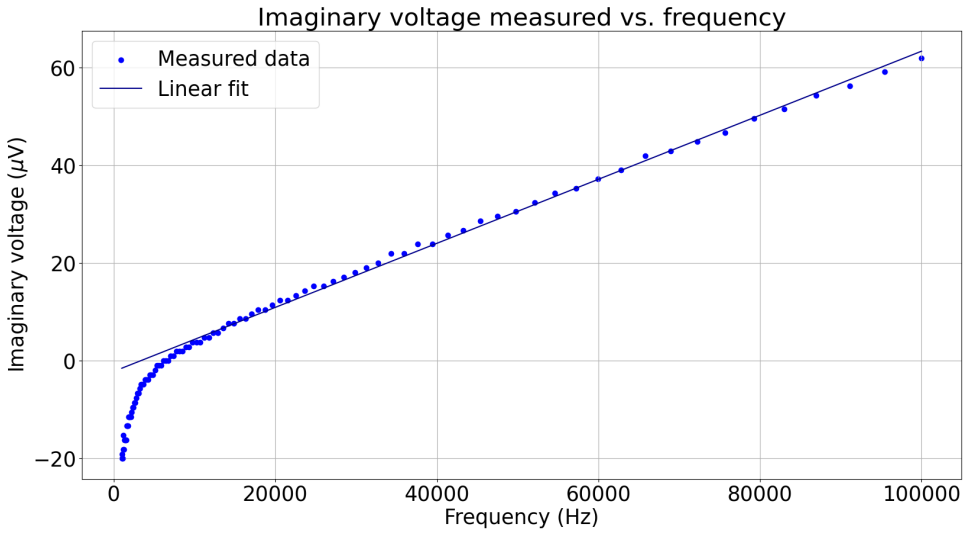

Figure 4.5: *Logarithmic frequency sweep from 0 Hz to 100 kHz. The linear fit has the following equation:* $V = 6.553 \cdot 10^{-10} f - 2.178 \cdot 10^{-6}$. *Note that this equation implies that there is a negative imaginary voltage at a frequency of 0 Hz. This is wrong and is caused by the erroneous offset caused by the initial negative values we omit from the linear fit. I will go further into detail about this fit in the discussion section.*

To determine the the inductance of the coil in superconducting state, we did a frequency sweep over one of the flux concentrator coils (figure 4.5). We used a linear fit, because the slope of the resulting curve is the inductance as I is constant (equation 2.3, equation 2.5). Using equation 2.6, we can assume that the inductance can never be negative. Therefore we attribute the negative values of Im(V) to an unknown offset. We used only the positive values for the linear fit.

The slope of the linear fit is 6.553e-10 which would mean the inductance of the superconducting coil is 655.3 pH. This is a large decrease in inductance from the 'normal' inductance of 360 μH. The decrease is in the order of 1e6, much more than expected from equation 2.6. We believe this is the case, because the assumption of an infinitely long solenoid is used for equation 2.6. This assumption falls apart when the flux concentrator is not applicable to the flux concentrator when it is in superconducting state.

4.2 Hall effect measurements

Due to the similar T_c of Nb and NbTi, we were not able to measure the superconducting transitions separately from each other. That's why we decided to do additional tests to make sure the niobium core is superconducting using a Hall effect sensor. In figure 4.6 the results of two current sweeps are visible, one at room temperature and one at 4.5 K. If we use equation 2.10, we would expect an amplification of the magnetic field given by $\frac{L_2}{L_1}$. In our case that would give an amplification of about 10. It is clearly visible in figure 4.6 that such an amplification is not nearly reached, in fact, there is no amplification but an attenuation.

In another test we did find signs that point to the niobium core being superconducting. In figure 4.7 the measured hall voltage is plotted over time together with the temperature of the cryostat. For the first part of the measurements the cryostat was at 4.5 K. We had the Tenma current source turned on at 100 mA with a compliance of 16 V without the feeding wire plugged in. This meant that the Tenma would experience an infinite resistance and therefore try to send a current with a voltage of 16 V. When plugging the wire back in, the Tenma would send this current for a split second before lowering the voltage to send the desired 100 mA. This would thus create a very short shock of very high current. When giving these shocks, the measured Hall voltage would be far greater than expected at 100 mA

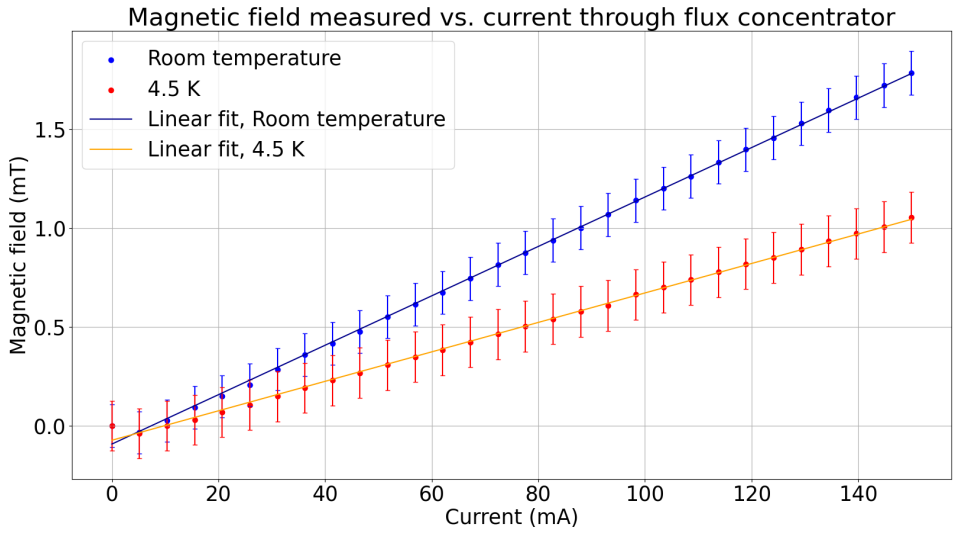

Figure 4.6: *Two current sweeps from 0 to 150 mA. The magnetic field is calculated by first subracting the voltage measured at 0 mA as this is assumed to be caused by external field and afterwards using a conversion factor of 0.2 V/T (from [18]), we do not know for sure that this conversion factor is applicable at cryogenic temperatures. The errorbars were calculated using the given 0.2% errormargin of the multimeter (Agilent 34410A) of the value measured before the offset was subtracted. The linear fit at room temperature has the following equation:* $B = 1.249 \cdot 10^{-2} I - 9.217 \cdot 10^{-5}$*. The linear fit at 4.5 K can be described with this equation:*$B = 7.449 \cdot 10^{-3} I - 7.287 \cdot 10^{-5}$*. Both of these equations imply there to be a negative magnetic field present at 0 mA. This is wrong and caused by an erroneous offset. In the discussion this offset is discussed in depth.*

which would remain even after unplugging the feeding wire again. This implies a persistent current was created with the shock which would only be possible if the niobium core was superconducting. This explanation is further supported by the fact that when warming up such that $T > T_c$, the measured hall voltage returns to it's expected position when no current is sent. When sending the same shocks through the coils with the niobium in 'normal' state, the measured hall voltage behaves as expected. The change in measured voltage corresponds to what we expect when sending 100 mA and the voltage returns back to the value we expect when unplugging the feeding wire.

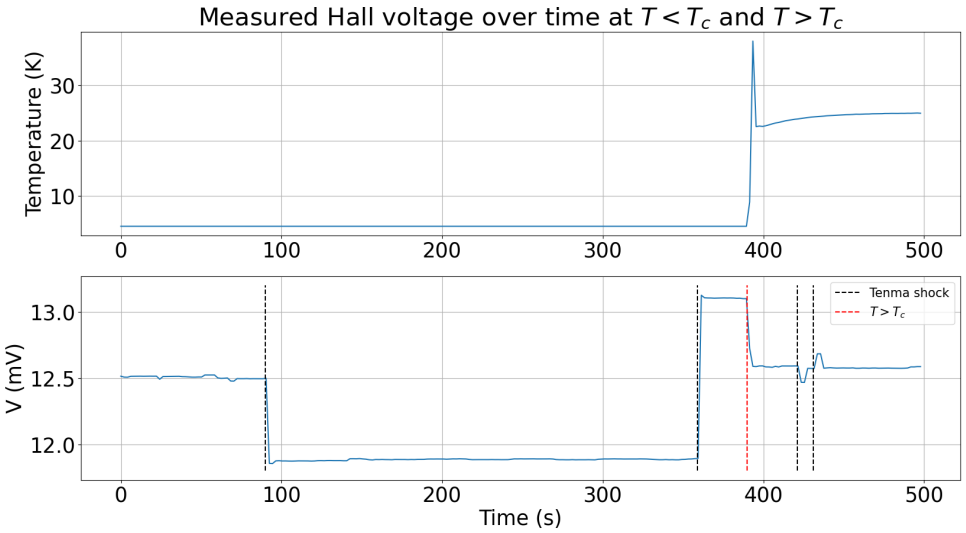

Figure 4.7: *The measured Hall voltage over time. The dashed black lines correspond to moments when we sent a large current shock through the coil. When $T < T_c$, the shocks result in a large change in measured voltage. After warming up such that $T > T_c$ (to the right of the red dashed line), the same shocks result in much smaller changes which do not persist after unplugging the current source.*

4.3 Levitation tests

Having gathered the results described above, the logical next step was to actually try and trap the microsphere and levitate it. These attempts were not successful. We did, however, gather some interesting results about the setup which we will now discuss.

(a) ***(b)*** ***(c)***

Figure 4.8: *(a): Two microspheres loaded in the sample holder, one is loaded on the glass and one on the copper foil. (b): The trap now with niobium debris fallen into it. (c): 4.8b after sending a large current shock through a flux concentrator. Note that the debris has moved slightly, contrary to the microspheres partially hidden by the fallen debris.*

Early in our attempts to trap the microsphere, we found that the loaded microsphere would not come loose from either the glass or the foil. We expected that it would be relatively simple to knock the microsphere loose, as it was only held in place by the weak Van der Waals force. The microspheres were most likely quite sticky due to the fact that they were dissolved in acetone before they were loaded into the sample holder. The acetone cleans them which is beneficial, however when acetone dries out, it leaves some residue. This residue probably caused the microspheres to be sticky even though they were cleaned. This problem was solved by dissolving the microspheres in isopropanol (IPA). This cleans the spheres less thoroughly, but leaves less residue when drying. After this change the microspheres came loose without difficulties when driving the piezo.

A different problem that came up, is the buildup of niobium debris which falls into the trap (figure 4.8). This debris starts to fall into the trap when cooling down, suggesting that it forms due to the contracting of the sample holder while the temperature is dropping. This is further substantiated by the fact that vibrating the piezo for long amounts of time (30 minutes) at room temperature, no debris buildup is visible. We know that the debris is niobium that came loose from the coils. We know this because when sending similar current shocks with the Tenmas as previously described with the piezo turned off, the debris moves. This means that the particles react to magnetic fields and thus are superconducting, assuming that no permanent magnetic particles have made their way into the setup. The only superconducting material which can make their way into the trap is niobium from the coils. An interesting detail is that even though the microspheres have been knocked loose by the piezo, they do not move when sending

current shocks like the niobium particles do. This may imply that they are not superconducting and may be the reason why the microspheres fail to levitate.

Chapter 5

Discussion

Having gathered all the results it is now time to critically discuss them. We will start with the most important question: why did we fail in trying to levitate the microsphere? After we discussed this we will go into detail about the specifics of the lock-in and Hall effect measurements.

5.1 Levitation tests

Unfortunately, we didn't succeed in trapping and stably levitating a microsphere. We believe this is caused by one of two reasons (or a combination of the two). First, we suspect that the microspheres do not reach superconducting temperatures of 7.5 K. This means that no Meissner effect occurs in the microsphere and therefore they are not affected by the created magnetic fields. This is supported by the fact that sending current shocks will cause the niobium particles to move, but the microsphere will stay stationary. This would imply that the thermalization of the microspheres is not sufficient. This is supported by the fact that when we used a niobium microsphere (with a T_c higher than that of SnPb) loaded on the glass instead of a SnPb one. it also did not move.

This is quite unexpected as copper is a great thermal conductor. In [7] the microsphere is loaded in a polylactide (a kind of plastic) bowl glued to the bottom coil. Polylactide has a thermal conductivity of 0.183 W/mK [19]. This is lower than the thermal conductivity of glass (0.9-1.2 W/mK [20]) and much lower than that of copper (413 W/mK [21]) so our microspheres should be thermalized well enough to reach the desired temperature. However, in [7] the experiment is done at millikelvin temperatures

in a dilution refrigerator, whereas we only reach a temperature of 4.5 K in our flow cryostat.
It might also be possible that T_c is reached, but the critical field H_c is exceeded. We never thoroughly investigated the critical field of the microspheres as it was hard to find a definitive value, but it could very well be that the critical field in our setup was very low due to the dependency of the temperature (equation 2.7). The minimal temperature reached inside the cryostat was 4.5 K. The critical temperature of the microspheres is 7.5 K. This means that H_c is at most 64% of the critical field at 0 K and could very well be less due to a probable higher temperature of the microsphere. If one would want to investigate the breaking of the superconductivity because the critical field is exceeded, the equations found in [22] would be very useful. They can be used to calculate the exact magnetic field generated by a coil as a function of x, y and z. This can lead to a better understanding of limits of the flux concentrator coil.

The second explanation of our setup working improperly ties in with the results shown in figure 4.6. The Hall sensor current sweeps did not confirm any noticeable amplification of the created magnetic field. This made us realize that we do not know for sure whether the flux concentrator coil actually works as we believe it does. There might even be the possibility that the design of the flux concentrators actually shields the microsphere from the generated magnetic field.

When a normal metal is in contact with a superconducting one, a tiny piece of the normal metal also becomes superconducting. This is called the proximity effect. This is the case in our setup: the niobium cores are in contact with the copper base. It could have been possible that the surface currents travelled through the superconducting copper to circumvent the slit made in the coils. This would mean the surface currents would not travel like it is shown in figure 2.3 and as a result do not generate the desired amplified field. At a late stage of the project we have sawed out a slit in both the copper base and top plate to see if it made any difference, but these measurements were inconclusive.

As a follow up research project, it would be wise to test the above stated problems. As a start it would be wise to thoroughly research the flux concentrator coils themselves. We did not have the proper understanding of the coils to make the right decisions during our research. This also applies to the microspheres. Accurately measuring their critical temperature and critical magnetic field is key in moving forward. Furthermore, placing the

setup in a dilution refrigerator to reach lower temperatures might be essential for reaching the needed superconducting temperatures for the microspheres. One could experiment with normal coils before trying again with flux concentrator coils. It should be possible to create a strong enough gradient to trap the microspheres with regular coils.

5.2 Superconducting tests

We will finally look at the results we did gather but do not fully understand or have some doubts about. Firstly let us look at the plot in figure 4.5. We fitted a linear function to the data, because we expected a linear dependency. However there is a clear domain in which the dependency is not at all linear and even gives (presumably impossible) negative values for the imaginary voltage. We saw the same behaviour in comparable sweeps we did, but found an expected positive value when doing the lock in measurements while cooling down (figure 4.4). For the measurements we did when cooling down we sent an alternating current with frequency of 1 kHz, well in the domain where during the sweep we measured a negative voltage. Why exactly the results are negative at lower frequencies while sweeping is unclear. A possible hypothesis would be that a high capacitance in the circuit might show up in imaginary voltage measurements as a negative voltage. We have not taken this into consideration during measurements and such have not measured the capacitance of the circuit.

In figure 4.6, we also have some negative measurements which are not expected. However, these can be partially explained. Before we plotted and fitted a linear function to the data, we subtracted the value of the first measurement where the current is 0 A. The magnetic field measured at this current is caused by external magnetic fields and therefore can be subtracted from the measured field generated by the coil. However, the field measured at 0 A was not the lowest measured value. Therefore when subtracting the presumed offset, one negative value was 'created'. The dip after the first measurement occurs in both the room temperature and 4.5 K sweep, implying that it is not a fluke but something structural. This structural error is probably caused by some measurement artefact, because when manually ramping the current through the flux concentrator coil we never see a decrease in magnetic field strength. The decrease only happens when measuring using the sweep script.

Lastly, it is possible that the measured attenuation in magnetic field is caused by the placement of the Hall effect sensor. If the flux concentrator does work as expected, the actual space in which the amplified magnetic field is at its strongest is very small. Furthermore, the Hall effect sensor has a specific spot where it is most sensitive for magnetic fields. It might very well be possible that the sensor was not perfectly aligned with the hole of the coil and therefore was unable to measure the strongest part of the amplified magnetic field. On the other hand, we found that when holding a small permanent magnet (250 μm) near the sensor the measured field by the Hall effect sensor was much smaller than when holding a larger magnet close to it, even though both magnets have the same magnetization. This might imply that the sensor is not suitable for measuring magnetic fields which take up little space, which is exactly what we are trying to do. A smaller sensor might be used to make sure it measures at the right place, for example a superconducting quantum interference device (SQUID).

Chapter 6

Conclusion and outlook

We have shown in this project that there is great potential in the proposed double-flux concentrator trap in anti-Helmholtz configuration. We constructed an experimental setup in which it is possible to send currents of 600 mA in a flow cryostat without breaking the superconducting state of the wire and coils. We did this by using heatsinks in the form of copper bobbins which are in great thermal contact with the flow cryostat around which the feeding wires are tightly wound. During the project we also proved the merit of using a relatively warm flow cryostat as opposed to a dilution refrigerator. The flow cryostat cools down in only 10 minutes, meaning the iteration rate of the setup is much higher than what would be possible if we used a dilution refrigerator, which takes a few days to cool down.

However, we have probably exhausted the possibilities of the current setup. It has a some shortcomings which need to be addressed and maybe even redesigned before it can be successful. The flow cryostat has its advantages, but to reach the desired temperatures for the microspheres to become superconducting, the lower temperatures inside a dilution refrigerator are most likely necessary. Furthermore, the flux concentrator coils need to be much better understood than they are now. We have made progress in our understanding of the flux concentrator coil, but much is still unclear. The results imply the the coils do become superconducting, but conclusive proof the magnetic field is concentrated and amplified is not found. Attempting the experiment using regular coils is a logical next step. This way it is possible to first focus on making sure the microspheres reach the proper temperature, before implementing the flux concentrator coils again.

Chapter 7

Acknowledgements

I would like to thank the Hensen group for the opportunity to work on my own project for four months. I felt supported in experimenting and making my own decisions while still being able to ask all the questions I had. Many thanks in particular to Bas for all the good ideas and encouraging me to keep trying when things would not work the first time (or the second time). Many thanks to Martijn for helping me with all my measurements and always being available for questions or just a chat. Thanks to the other bachelor students Mart, Job, Jasper and Matthijs and everyone else in both the Hensen and Oosterkamp groups for making sure the lab is a very 'gezellig' work environment where there is plenty of space to have a laugh besides the serious work (and therefore keeping me sane).

Bibliography

[1] R. S. Schappe and C. Barbosa, *A simple, inexpensive acoustic levitation apparatus*, The Physics Teacher **55**, 6 (2017).

[2] A. Ashkin, *Acceleration and Trapping of Particles by Radiation Pressure*, Physical Review Letters **24**, 156 (1970).

[3] G. Pesce, P. H. Jones, O. M. Marago, and G. Volpe, *Optical tweezers: theory and practice*, The European Physical Journal Plus **135** (2020).

[4] W. Jones, *Earnshaw's theorem and the stability of matter*, European Journal of Physics **1**, 85 (1980).

[5] W. Paul and H. Steinwedel, *Notizen: Ein neues Massenspektrometer ohne Magnetfeld*, Zeitschrift fur Naturforschung. A, A Journal of Physical Sciences **8**, 448 (1953).

[6] M. Perdriat, C. Pellet-Mary, T. Copie, and G. Hetet, *Planar magnetic Paul traps for ferromagnetic particles*, Physical Review Research **5** (2023).

[7] J. Hofer, R. Gross, G. Higgins, H. Huebl, O. Kieler, R. Kleiner, D. Koelle, P. Schmidt, J. A. Slater, M. Trupke, K. Uhl, T. Weimann, W. Wieczorek, and M. Aspelmeyer, *High- Q Magnetic Levitation and Control of Superconducting Microspheres at Millikelvin Temperatures*, Physical Review Letters **131** (2023).

[8] G. Jin, A. Luo, Y. Chen, and H. Xiao, *Expansion of the Ohm's Law in Nonsinusoidal AC Circuit*, 2015.

[9] J. Bardeen, L. N. Cooper, and J. R. Schrieffer, *Theory of Superconductivity*, Physical Review **108**, 1175 (1957).

[10] M. Tinkham, *Introduction to Superconductivity*, Courier Corporation, 2004.

[11] J. E. Hirsch, *On the dynamics of the Meissner effect*, Physica Scripta **91**, 035801 (2016).

[12] A. Abrikosov, *Nobel Lecture: Type-II superconductors and the vortex lattice*, Reviews of mMdern Physics **76**, 975 (2004).

[13] B. Goodman, *Type II superconductors*, Reports on Progress in Physics **29**, 445 (1966).

[14] Testbook, *Superconductivity: meaning, types of superconductors, formulae https://testbook.com/physics/superconductivity*, 2023.

[15] F. C. Moon, *Superconducting levitation : applications to bearings and magnetic transportation*, 1994.

[16] J. Plugge, *Generating high B0 -fields for use in extremely low temperature MRFM*, 2020.

[17] Lake shore Cryotronics, *Model ST-500 and ST-500-C SuperTran System Operating Instructions*, Technical report, 2023.

[18] Asensor Technology AB, *Linear High Precision Analog Hall Sensor HE144*, Technical report.

[19] G. Spinelli, R. Kotsilkova, E. Ivanov, V. Georgiev, C. Naddeo, and V. Romano, *Thermal and Dielectric Properties of 3D Printed Parts Based on Polylactic Acid Filled with Carbon Nanostructures*, Macromolecular Symposia **405** (2022).

[20] Schott, *TIE-31: Mechanical and thermal properties of optical glass*, Technical report, 2004.

[21] Editor Engineeringtoolbox, *Metals, metallic elements and alloys - thermal conductivities https://www.engineeringtoolbox.com/thermal-conductivity-metals-$d_8$58.html*, 2024.

[22] J. C. Simpson, NASA, J. E. Lane, I. Dynacs, C. D. Immer, I. Dynacs, R. C. Youngquist, and NASA, *Simple analytic expressions for the magnetic field of a circular current loop*, Technical Report NASA/TM-2013-217919, 2001.